Early suppression of excitability in subcortical band heterotopia modifies epileptogenesis in rats

Delphine Hardy, Emmanuelle Buhler, Dmitrii Suchkov, Antonin Vinck, Aurélien Fortoul, Françoise Watrin, Alfonso Represa, Marat Minlebaev, Jean-Bernard Manent

Neurobiology of Disease 177 (2023) 106002

Contents lists available at ScienceDirect

Neurobiology of Disease

journal homepage: www.elsevier.com/locate/ynbdi

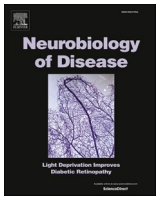

Early suppression of excitability in subcortical band heterotopia modifies epileptogenesis in rats

Delphine Hardy [1], Emmanuelle Buhler [1], Dmitrii Suchkov [1], Antonin Vinck, Aurélien Fortoul, Françoise Watrin, Alfonso Represa, Marat Minlebaev, Jean-Bernard Manent [*]

INMED, INSERM, Aix-Marseille University, Turing Centre for Living Systems, Marseille, France

ARTICLE INFO

Keywords:
Malformation of cortical development
Grey matter heterotopia
Rodent model
Epileptogenesis
Epilepsy

ABSTRACT

Malformations of cortical development represent a major cause of epilepsy in childhood. However, the pathological substrate and dynamic changes leading to the development and progression of epilepsy remain unclear. Here, we characterized an etiology-relevant rat model of subcortical band heterotopia (SBH), a diffuse type of cortical malformation associated with drug-resistant seizures in humans. We used longitudinal electrographic recordings to monitor the age-dependent evolution of epileptiform discharges during the course of epileptogenesis in this model. We found both quantitative and qualitative age-related changes in seizures properties and patterns, accompanying a gradual progression towards a fully developed seizure pattern seen in adulthood. We also dissected the relative contribution of the band heterotopia and the overlying cortex to the development and age-dependent progression of epilepsy using timed and spatially targeted manipulation of neuronal excitability. We found that an early suppression of neuronal excitability in SBH slows down epileptogenesis in juvenile rats, whereas epileptogenesis is paradoxically exacerbated when excitability is suppressed in the overlying cortex. However, in rats with active epilepsy, similar manipulations of excitability have no effect on chronic spontaneous seizures. Together, our data support the notion that complex developmental alterations occurring in both the SBH and the overlying cortex concur to creating pathogenic circuits prone to generate seizures. Our study also suggests that early and targeted interventions could potentially influence the course of these altered developmental trajectories, and favorably modify epileptogenesis in malformations of cortical development.

1. Introduction

Epileptogenesis refers to the development and extension of tissue capable of generating spontaneous seizures, resulting in the development of an epileptic condition and/or the progression of the epilepsy after it is established (Pitkänen et al., 2013). Various acquired or genetic factors can trigger epileptogenesis, and, accordingly, there is a wide spectrum of epilepsy syndromes, each of them characterized by distinct etiologies, natural course of disease and underlying pathological mechanisms. Identifying the dynamic changes occurring during the course of epileptogenesis in order to prevent, ameliorate, or cure epilepsy is a major challenge for epilepsy research (Galanopoulou et al., 2021).

Disrupted formation of the cerebral cortex represents a major cause of epilepsy in childhood, and malformations of cortical development (MCDs) account for up to 40% of intractable or drug-resistant cases (Leventer et al., 2008). MCDs comprise a large group of structural brain abnormalities, with genetic and non-genetic underlying causes, and variable clinical presentations and burden of disability. One can broadly distinguish two main groups: early-onset and diffuse MCDs, generally associated with poor neurological outcomes, and late-onset, more focal MCDs, associated with milder outcomes (Guerrini and Dobyns, 2014). Because MCDs are usually not detected until patients begin having epileptic seizures, our understanding of epileptogenesis in MCDs remains limited.

Subcortical band heterotopia (SBH) belongs to the group of diffuse

Abbreviations: ElectroCorticoGram, ECoG; DCX, doublecortin; Dcx-KD, doublecortin knockdown; FCD, focal cortical dysplasia; MCD, malformations of cortical development; PVNH, periventricular nodular heterotopia; SBH, subcortical band heterotopia; NCx, normotopic cortex; shRNA, short hairpin RNA; SW, spike-and-wave; SWD, spike-and-wave discharge.

* Corresponding author at: INMED, 163 Route de Luminy BP13, 13273 Marseille Cedex 09, France.
E-mail address: jean-bernard.manent@inserm.fr (J.-B. Manent).

[1] These authors contributed equally to this work.

https://doi.org/10.1016/j.nbd.2023.106002
Received 10 October 2022; Received in revised form 4 January 2023; Accepted 13 January 2023
Available online 14 January 2023

MCDs (Bahi-Buisson and Guerrini, 2013), and is characterized by a band of grey matter separated from the cortex and lateral ventricles by zones of white matter (Barkovich et al., 1989; Dobyns, 2010). DCX mutations are the most frequently diagnosed genetic causes for SBH, accounting for 100% of familial cases and over 80% of sporadic cases (Matsumoto et al., 2001; Bahi-Buisson et al., 2013). Patients with SBH present with mild to moderate intellectual disability (68% of cases), seizures (85–96%), including a high proportion of drug-resistance (78%) (Bahi-Buisson et al., 2013; Tanaka and Gleeson, 2008). Although our understanding of the pathophysiology of epileptogenic MCDs, has greatly improved (Represa, 2019), both the epileptogenic substrate and dynamic changes occurring during the course of epileptogenesis remain largely elusive, especially in severe and diffuse cases of MCDs such as SBH.

Here, we characterized the age-dependent evolution of electrographic discharges during epileptogenesis in an etiology-relevant rat model of SBH (Sahu et al., 2019) using longitudinal electrocorticographic monitoring. We found that epilepsy gradually progresses with age, with both quantitative and qualitative changes of seizure properties and patterns. We also dissected the relative contribution of the SBH and the overlying cortex to the development and age-dependent progression of epilepsy using a targeted approach for suppressing neuronal excitability. We report that an early suppression of neuronal excitability in SBH slows down epileptogenesis in juvenile rats, whereas epileptogenesis is paradoxically exacerbated when excitability is suppressed in the overlying cortex. However, in rats with active epilepsy, similar manipulations of excitability have no effect on chronic spontaneous seizures. Together, these findings suggest that complex developmental alterations occurring in both the SBH and the overlying cortex concur to creating pathogenic circuits prone to generate seizures. Our study also suggest that early and targeted interventions could potentially influence the course of these altered developmental trajectories, and favorably modify epileptogenesis.

2. Materials and methods

2.1. Animal ethics

Animal experiments were performed in agreement with European directive 2010/63/UE and received approval [2020080610441911_v2 (APAFIS#26835)] from the French Ministry for Research after ethical evaluation by the Institutional Animal Care and Use Committee of Aix-Marseille University.

2.2. Tripolar in utero electroporation

We performed tripolar in utero electroporation as described (Sahu et al., 2019; Moustaki et al., 2019). Timed pregnant Wistar rats (Janvier) received buprenorphine (Buprecare, 0.03 mg/kg) and Carprofen (Rimadyl, 5 mg/kg) and were anesthetized with isoflurane (2.5%) 30 min later. Uterine horns were exposed under isoflurane anesthesia, and plasmid vectors (plasmid conditions, Supplementary Figs. 1 and 5) were microinjected bilaterally into the lateral ventricles of embryonic day 16 embryos, together with fast green dye. Tripolar electroporations were accomplished by delivering 50 V voltage pulses (BTX ECM830 electroporator; Harvard Apparatus) across tweezer-type electrodes laterally pinching the head of each embryo through the uterus, and a third electrode positioned at the brain midline (Supplementary Fig. 1A). Successfully electroporated rats were selected one day after birth (P1) based on fluorescent protein expression by using transcranial illumination.

2.3. Telemetric electrocorticographic recording

We performed telemetric recordings of electrocorticographic signals (ECoG) in freely behaving, unrestrained Dcx-KD rats as described (Sahu et al., 2019). Juvenile bilateral Dcx-KD rats received buprenorphine (Buprecare, 0.03 mg/kg) and Carprofen (Rymadyl, 5 mg/kg) and were anesthetized with isoflurane (induction 5%, maintenance 2–3%) 30 min later. Rats were placed in a stereotaxic frame (Kopf Instruments) and 2 holes were drilled through the skull above somatosensory cortex for electrode implantation using coordinates relative to Bregma (AP:-0.5, L:+3.5). Reference electrode was placed on the cerebellum (AP:-10, L:+1.4). Electrodes were secured with screws and mounted with dental acrylic. A subcutaneous pocket was created to insert the telemetry transmitter (CTA—F40, Data Sciences International) on the left dorsal side of the rat. ECoG signals were digitized with Ponemah software (recording schedule as in Fig. 2).

2.4. Seizure detection

ECoG signals were processed as follows (Supplementary Fig. 2): 1) we extracted 150 ms segments every 10 ms, 2) we normalized amplitudes and extracted mean values from the normalized signal, 3) we calculated velocities, 4) we generated 50 by 50 matrices and filled them with the paired values of amplitude/velocities calculated for every ECoG segments. 5) We vectorized the resulting images depicting the phase portraits of individual segments to generate the input dataset.

Because we found that the phase portraits of SWs were distinct to that of rhythmic waves or background noise (Fig. 1E2, 1F), we used their characteristic shapes as alphabet characters to develop a seizure detection framework based on a character recognition approach. We used a neural network with 112 hidden layers and cross entropy parameter for the network performance estimation. The training dataset was composed of 38,911 events (34,485 noise events, 2,162 rhythmic waves and 2,264 SWs) that we manually selected using threshold methods and visual inspection. After training, the trained neural network was then used to detect seizures on the target dataset generated from ECoG signals processed similarly (Supplementary Fig. 2B).

2.5. Seizure analysis

We defined a seizure episode as a sequence of SW complexes with inter-event intervals shorter than 500 ms. If intervals were longer than 500 ms, we considered that a new seizure episode has started. Only seizures with durations >1 s were used for further analysis. For every detected seizures, we extracted peak values as follows: 1) We detrended seizures from their low frequency components (less 1 Hz); 2) We smoothed seizures with a 10 ms window; 3) We extracted phase components using Hilbert transformation; 4) We identified points with rapid changes in phase, which corresponds to peaks position. For each peak, we calculated time-stamp, amplitude and half-width.

2.6. Slice electrophysiology

P13 to P16 rats were deeply anesthetized with tiletamine/zolazepam (Zoletil, 40 mg/kg) and medetomidine (Domitor, 0.6 mg/kg), and decapitated. The brain was then quickly removed and was placed in chilled and oxygenated ACSF containing the following (in mM): 25 NaHCO3, 1.25 NaH2PO4.H2O, 6.3 D-glucose, 2.5 KCl, 7 MgCl2.6H2O, 0.5 CaCl2.2H2O and 132.5 choline chloride. Coronal slices (250-μm-thick) were obtained using a vibrating microtome (Leica Biosystems). During the electrophysiological experiments, the slices were superfused with oxygenated ACSF at a rate of 2 ml/min containing the following (in mM): 126 NaCl, 26 NaHCO3, 1.2 NaH2PO4.H2O, 6.3 D-Glucose, 3.5 KCl, 1.3 MgCl2.6H2O, 2 CaCl2.2H2O. Recordings were amplified using a Multiclamp 700B amplifier (Molecular Devices) and digitized using a Digidata 1440A (Molecular Devices). Patch electrodes (ranging from 6 to 9 MΩ) were filled with intracellular solution containing (in mM): 120 KMeSO4, 10 KCl, 10 HEPES, 8 NaCl, 4 Mg-ATP, 0.3 Na-GTP, and 0.3 Tris-base. The intracellular solution was also supplemented with 5 mM of biocytin to ensure cell morphological reconstruction.

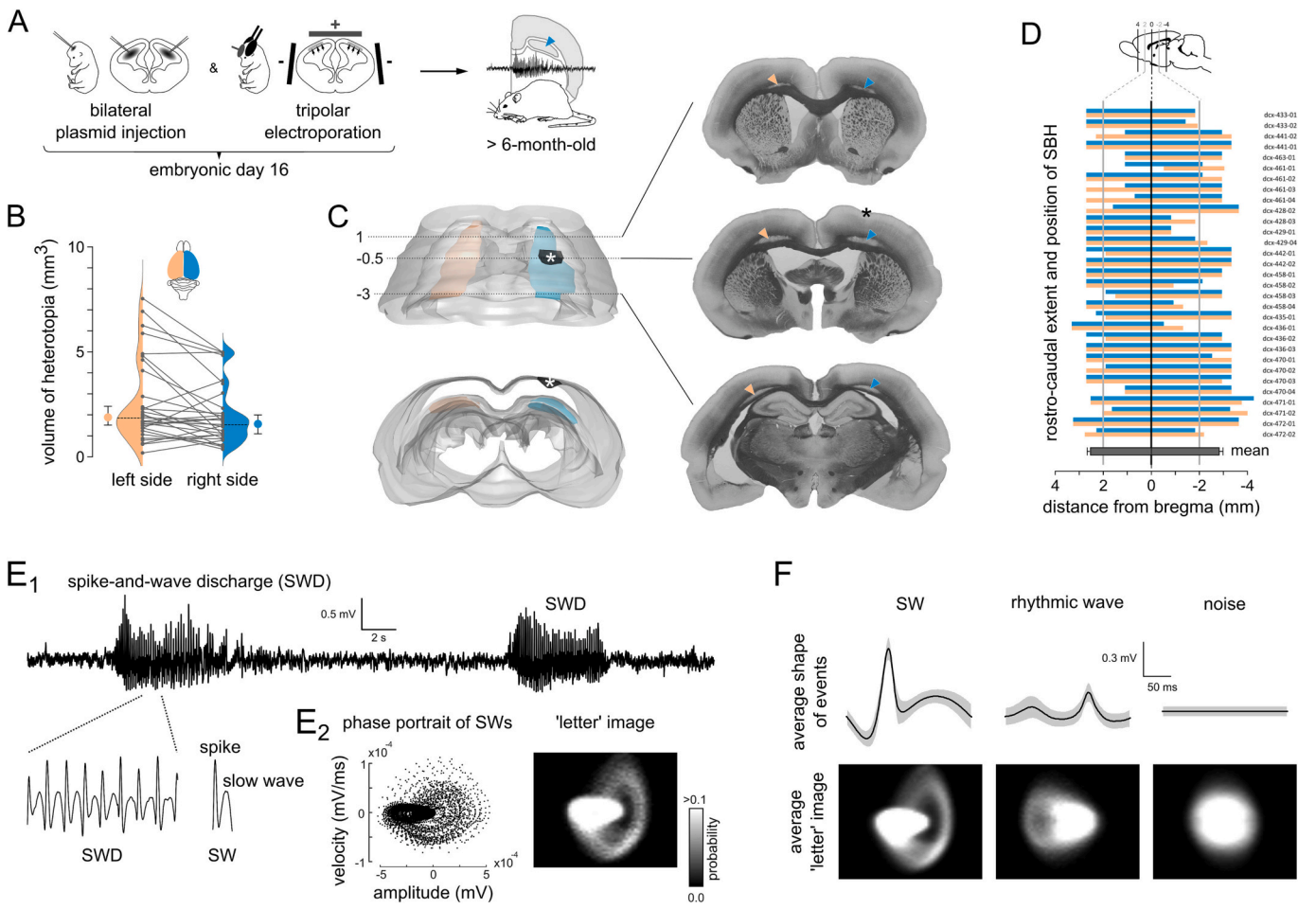

Fig. 1. Adult bilateral Dcx-KD rats harbor bilateral SBH and chronic spontaneous seizures. (A) Experimental timeline. **(B)** Line graphs and density estimates showing the volume of SBH in the left (orange) and right (blue) hemispheres of 31 adult bilateral Dcx-KD rats. Grey dots correspond to individual values, with the left and right values for individual rats connected with a line. Dashed lines on the density plots show medians. Orange and blue circles with error bars show medians and 95% confidence intervals. **(C)** Top view (top) and rear view (bottom) of the rostral part of a three-dimensionally reconstructed adult brain with bilateral SBH (in orange in the left hemisphere, in blue in the right hemisphere). (right) 3 frontal sections taken at the indicated positions from bregma showing the band heterotopia (orange and blue arrowheads) in the white matter (in dark grey). Asterisks indicate the electrode implantation site. **(D)** Clustered bar graphs showing the rostrocaudal extent and position of SBH relative to bregma in the 31 bilateral Dcx-KD rats analyzed, in the left (orange) and right (blue) hemispheres. Dark grey bar shows the mean values with SEM. Animal identifier codes are given next to each pairs of bars. **(E1)** Representative ECoG trace showing two spike-and-wave discharges (SWD), composed of trains of spikes (S) followed by associated slow waves (W), and referred to as spike-and-wave (SW) complexes. **(E2)** Phase portrait of 1000 SWs (left) and corresponding 'letter' image. **(F)** Average traces of SW, rhythmic wave and noise, and corresponding 'letter' image of their phase portraits. (For interpretation of the references to colour in this figure legend, the reader is referred to the web version of this article.)

2.7. Histology

Animals were deeply anesthetized with tiletamine/zolazepam (Zoletil, 40 mg/kg) and medetomidine (Domitor, 0.4 mg/kg) and perfused transcardially with 4% paraformaldehyde. Serial frontal sections (100 µm) were performed using a vibrating microtome (Leica Biosystems) and mounted on glass slides. Images were taken using a fluorescence stereomicroscope (Olympus) and a wide-field microscope equipped with a structured illumination system (Zeiss). Measurements and tridimensional brain reconstructions were performed using Free-D (Andrey and Maurin, 2005).

2.8. Statistics

To study the age-related progression of seizure parameters (number, duration, amplitude, proportion of spikes), we computed the best-fit regression lines of these parameters against age, and considered the steepness of the regression lines as a descriptor of how epilepsy progresses with age. In order to compare epilepsy progression among groups, we compared slopes and intercepts of these regression lines, and estimated the probability that the elevations of these lines are different. To compare the effect sizes of excitability manipulation on the quantified endpoints (numbers of seizures and proportion of spikes within cortical discharges in 5–6-month-old rats), we computed the mean differences and their bootstrap 95% confidence intervals, and used Cumming estimation plots, as described by Ho et al. (Ho et al., 2019) We performed statistical analyses with Prism 9 (GraphPad Software). Significance level was set at $P < 0.05$. We generated Cumming and Gardner-Altman estimation plots as described by Ho et al. (Ho et al., 2019) and Violin SuperPlots as described by Kenny and Schoen (Kenny and Schoen, 2021).

3. Results

3.1. Adult bilateral Dcx-KD rats harbor bilateral SBH and exhibit chronic spontaneous seizures

We studied bilateral Dcx-KD rats as a genetic model of malformation

of cortical development causing epilepsy. We generated cohorts of these rats using tripolar in utero electroporation, a method enabling targeted, bi-hemispheric genetic manipulations in the developing isocortex (Fig. 1A and Supplementary Fig. 1A, C). Adult bilateral Dcx-KD rats harbored prominent bilateral SBH extending rostrocaudally in the white matter and resembling that seen in humans (Fig. 1B-D), and exhibited chronic spontaneous non-convulsive seizures, as we reported earlier (Sahu et al., 2019). These seizures in adulthood consisted of spike-and-wave discharges (SWDs) composed of trains of spikes (S) followed by associated slow waves (W), and referred to as spike-and-wave (SW) complexes (Fig. 1 E1). No SWDs were detected, neither in sham-operated rats (injection only or tripolar electroporation only), nor in rats electroporated with ineffective shRNAs with mutations creating mismatches and harboring no SBH, thus confirming their epileptic nature, as we described earlier (Sahu et al., 2019). We found that the amplitude and velocity of amplitude of SW could serve as a unique descriptor of their electrographic signature (Fig. 1 E2), distinct to that of rhythmic waves or background noise (Fig. 1F). We thus developed an ad hoc seizure detection algorithm based on a character recognition approach utilizing these so-called phase portraits as alphabet characters (Supplementary Fig. 2A, B and Material and methods).

3.2. Epilepsy progresses with age in juvenile rats with bilateral SBH

To investigate the development and potential age-related changes of epileptiform activity in bilateral Dcx-KD rats, we performed longitudinal electrocorticographic (ECoG) recordings over a three-month period with implanted telemetric devices equipped with motion sensors (Fig. 2A). We used our seizure detection algorithm to quantify seizures occurring over 24-h periods, as well as their hourly counts, on a monthly basis from three to six months of age. We also quantified hourly motion counts, and examine their diurnal rhythmicity across the light-dark phase. Cosinor analysis of motion counts (Fig. 2B) confirmed that peaks of motion occurred in the dark phase at all ages, and that the rats showed significantly higher proportions of cumulated motion in the dark phase (median, 64.41% with 95% CI of median [60.68, 67.94], Fig. 2C), as expected from nocturnal animals. Hourly seizure counts however showed no clear rhythmicity and occurred in equal proportions in the light or dark phase (median, 48.82% with 95% CI of median [43.37, 50.41], Fig. 2C). Of note, the skewed distribution of inter-seizure intervals (Supplementary Fig. 3) showed that seizures often occurred in clusters.

We next evaluated the correlation between the age of the rats and the number of seizures occurring over a 24 h period, and with their duration or amplitude. We found significant positive relationships between the age and the number (Spearman $r = 0.4749$, $p = 0.0255$, Fig. 2D), the duration (Spearman $r = 0.530$, $p = 0.0111$, Fig. 2E) and the amplitude of seizures (Spearman $r = 0.5324$, $p = 0.0108$, Fig. 2F), suggesting an age-dependent evolution of seizures in bilateral Dcx-KD rats. Consistent with the pharmacological properties of SWDs in humans and rodent models, ethosuximide significantly reduced seizure numbers in six-month-old rats ($p = 0.0313$, Wilcoxon test, Fig. 2D), while the duration or amplitude of remaining seizures were unchanged (Fig. 2E, F). Last, we examined if the age-dependent changes in the number, duration and amplitude of seizures were associated with changes in their electrographic patterns. We quantified the proportion of spikes (vs. waves) within cortical discharges, plotted them as a function of seizure duration, and compared their distribution across ages. This analysis revealed that seizures gradually progresses from brief epileptiform discharges mostly composed of spikes in three-month-old bilateral Dcx-KD rats, to long-lasting fully developed SWDs composed of an equal proportion of spikes and waves from five months onward (Fig. 2G). We found a significant negative relationship between the age of the rats and the mean proportion of spikes within cortical discharges (Spearman $r = -0.5705$, $p = 0.0056$, Fig. 2H). We confirmed this observation by plotting both individual and pooled distributions of spike proportions per cortical discharges for individual rats and for the rats of the same age group (Fig. 2I). This revealed that, despite inter-individual differences, cortical discharges tended to comprise an equal proportion of spikes and waves by five months of age, and we considered that rats have reached a mature stage of SWDs.

Altogether, these observations indicate that epilepsy gradually progresses in juvenile rats with bilateral SBH, with prominent changes in the occurrence, duration and amplitude of seizures, and in the properties of their electrographic patterns.

3.3. Early targeted suppression of neuronal excitability in SBH and not in the normotopic cortex modifies epileptogenesis

To dissect the contribution of SBH and that of the normotopic cortex (NCx) to the development and age-dependent progression of epilepsy, we utilized a targeted molecular genetic approach for suppressing neuronal excitability (White et al., 2001). We created cohorts of bilateral Dcx-KD rats functionally expressing either in SBH, or in the NCx, an inwardly rectifying potassium channel, Kir2.1, that we and others have previously used to manipulate excitability (Burrone et al., 2002; Mizuno et al., 2007; Petit et al., 2014). We first confirmed with patch-clamp recordings that constitutive Kir2.1 expression in cortical neurons is associated with a significantly more hyperpolarized resting membrane potential than controls, consistent with a decreased excitability (mean difference, −18.36 mV, with 95% CI of mean [−24.49, −12.28], $p = 0.00008$, Mann-Whitney test, Supplementary Fig. 4).

We generated rats with SBH-targeted Kir2.1 expression (referred to as rats with silenced SBH in Fig. 3) by injection and tripolar co-electroporation of plasmids encoding GFP, Kir2.1 and Dcx shRNAs, respectively (Supplementary Fig. 5 A1, A2). Of the total population of Kir2.1-expressing cells, those located in the SBH ranged between 37.39% and 98.34% with this experimental setting (Supplementary Fig. 6A). We then longitudinally monitored the age-related changes of epileptiform activity in rats with silenced SBH using telemetric ECoG recordings and the same experimental timeline as for un-manipulated bilateral Dcx-KD rats. We used the same parameters as described above to describe seizure progression. We calculated the best-fit regression lines and used them to describe the progression of seizure parameters with age, and to compare bilateral Dcx-KD rats with silenced SBH and un-manipulated ones. We found that rats with silenced SBH tended to have lower slope and elevation values for the number of seizures over a 24 h period (elevation, $p = 0.0580$, Fig. 3 A1), their duration (elevation, $p = 0.0190$, Fig. 3 A2) and amplitude (elevation, $p < 0.0001$, Fig. 3 A3), and for proportion of spikes within cortical discharges (elevation, $p = 0.0123$, Fig. 3 A4). Plots of the proportion of spikes as a function of seizure duration across ages also revealed a slower progression towards fully developed SWDs (Fig. 3 A5). Because un-manipulated bilateral Dcx-KD rats harbor fully developed SWDs from five months onward, we compared the pooled numbers of seizures in five-six-month-old rats with silenced SBH to that of un-manipulated ones (Fig. 3C). We found that rats with silenced SBH had significantly lower numbers of seizures occurring over a 24 h period than un-manipulated controls (mean difference, −94.77 seizures, with 95% CI of mean difference [−183, −9.61], $p = 0.0360$, Mann-Whitney test). Last, the proportion of spikes within cortical discharges tended to be higher than that of un-manipulated Dcx-KD rats, suggesting a lower maturation pace of SWDs (mean difference, 0.11, with 95% CI of mean difference [−0.01, 0.21], $p = 0.0596$, Mann-Whitney test, Fig. 3D). These findings are consistent with a modified epileptogenesis in bilateral Dcx-KD rats with silenced SBH, characterized by a slower age-related increase of seizure numbers and a slower progression towards fully developed SWDs.

We next evaluated the effects of a similar manipulation in the normotopic cortex of bilateral Dcx-KD rats. To generate rats with NCx-targeted Kir2.1 expression (referred to as rats with silenced NCx in Fig. 3), we used tripolar in utero electroporation and a two-step

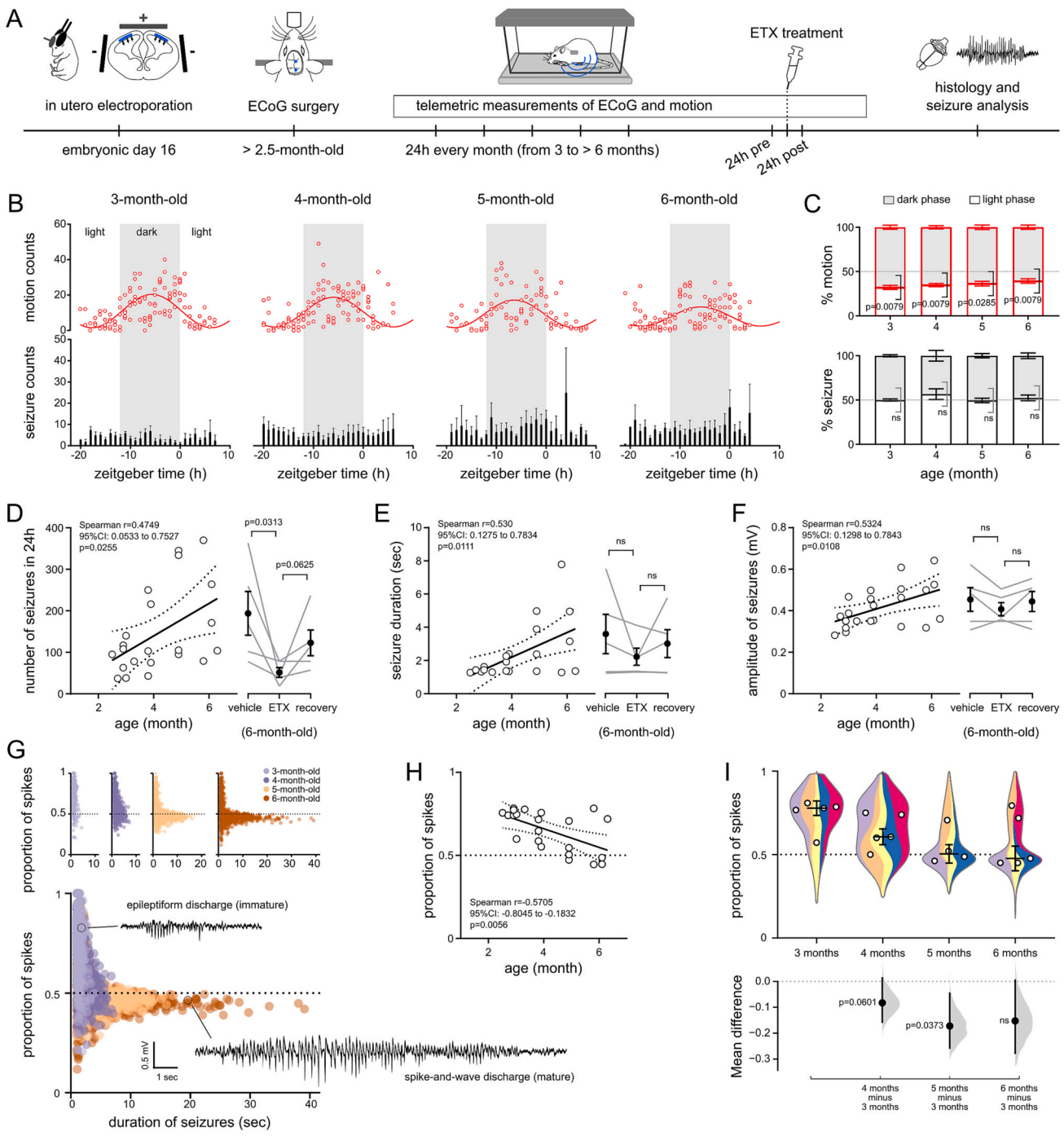

Fig. 2. Age-dependent progression of epilepsy in bilateral SBH rats. (A) Experimental timeline. **(B)** Upper graphs show dot plots of hourly motion counts, with superimposed sine waves representing the Cosinor analysis of motion across the light-dark phase. Lower graphs show bar graphs of hourly seizure counts. Error bars show SEM. **(C)** Stacked bar graphs showing the proportion of motion (top) and seizure (bottom) occurring during the dark and light phase. Error bars show SEM. **(D-F)** Number of seizures in 24 h (D, left), seizure duration (E, left) and amplitude (F, left) plotted as a function of age (in months), and best-fit linear regression lines. Open circles represent mean individual values, dotted lines show confidence intervals of the best-fit line. Line graphs showing the number of seizure in 24 h (D, right), seizure duration (E, right) and amplitude (F, right) after vehicle and ethosuximide (ETX) administration, and during the recovery period after ETX administration (post-ETX) in the 6-month-old group. Black dots and error bars show mean values and SEM. **(G)** Proportion of spikes within cortical discharges plotted as a function of seizure duration in 4 age groups. The 4 graphs are superimposed in B to show the progression from brief epileptiform discharges mostly composed of spikes in young bilateral Dcx-KD rats, to long-lasting spike-and-wave discharges composed of an equal proportion of spikes and slow waves in older bilateral Dcx-KD rats. **(H)** Proportion of spikes within cortical discharges plotted as a function of age (in months), and best-fit linear regression line showing an age-dependent progression of discharges patterns in bilateral Dcx-KD rats. Open circles represent mean individual values, dotted lines show confidence intervals of the best-fit line. **(I)** The upper graph shows violin superplots (top) of the proportion of spikes within cortical discharges in 4 age groups. Colored stripes show the normalized density estimates of individual discharges for each rat. Outlines show the overall density estimate of the age group. Open circles show median values for each rat, and horizontal lines and error bars show mean and SEM for the age group. The lower graph shows a Cumming estimation plot illustrating the mean difference compared to the 3 month age group. Mean differences are plotted as bootstrap sampling distributions (light grey areas), black dots and vertical error bars show mean difference and 95% confidence intervals.

procedure (Supplementary Fig. 1B). We first bilaterally injected and co-electroporated plasmids encoding mCherry and Kir2.1 to express these transgenes in the NCx; then, 30 min later, we bilaterally injected and co-electroporated plasmids encoding GFP and Dcx shRNAs to create bilateral SBH (Supplementary Fig. 5 B1, B2). Of the total population of Kir2.1-expressing cells, those located in the NCx ranged between 67.24% and 94.42% with this experimental setting (Supplementary Fig. 6B). We then longitudinally monitored the age-related changes of epileptiform activity with the same experimental and analysis pipeline as described above. We found that rats with silenced NCx had strikingly high numbers of seizures from 3 months onward, with no clear age-related evolution, suggesting that they had already reached a plateau number of seizures (Fig. 3 B1). The duration (Fig. 3 B2) and amplitude (Fig. 3 B3) of seizures remained similarly stable with age. Interestingly, the proportion of spikes within cortical discharges did not change with age, and remained in the range values of immature epileptiform discharges found in young un-manipulated Dcx-KD rats (Fig. 3 B4, 3B5). We compared the pooled numbers of seizures in five-six-month-old rats with silenced NCx to that of un-manipulated ones and found that rats with silenced NCx had significantly higher numbers of seizures occurring over a 24 h period (mean difference, 325.30 seizures, with 95% CI of mean difference [190.97, 493.90], $p = 0.0033$, Mann-Whitney test, Fig. 3C). Last, rats with silenced NCx had a significantly higher proportion of spikes within cortical discharges than that of un-manipulated Dcx-KD rats (mean difference, 0.18, with 95% CI of mean difference [0.08, 0.25], $p = 0.0141$, Mann-Whitney test, Fig. 3D). These findings are consistent with an exacerbated epileptogenesis in rats with silenced NCx, characterized by strongly increased numbers of epileptiform

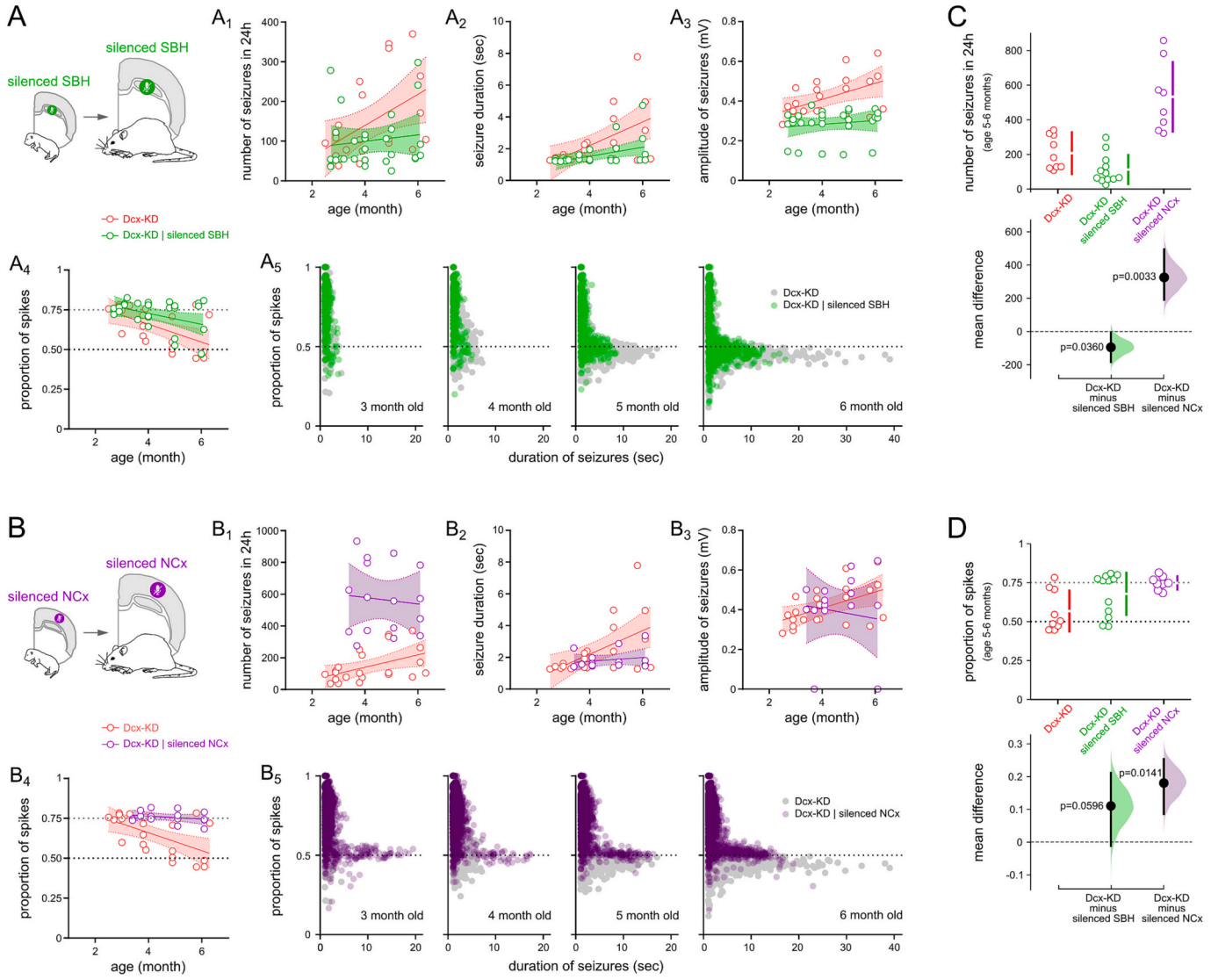

Fig. 3. Early chronic suppression of neuronal excitability in the SBH of bilateral Dcx-KD rats modifies epileptogenesis, whereas early chronic suppression of neuronal excitability in the normotopic cortex worsens it. (A, B) Schematic views of the experimental design. **(A1-A4, B1-B4)** Number of seizures in 24 h (A1, B1), seizure duration (A2, B2) and amplitude (A3, B3), and proportion of spikes within cortical discharges (A4, B4) plotted as a function of age (in months), and best-fit linear regression lines, in bilateral Dcx-KD rats (red) as compared to bilateral Dcx-KD rats with chronically suppressed neuronal excitability in SBH (silenced SBH, green) or in the normotopic cortex (silenced NCx, purple). Open circles represent mean individual values, shaded areas show confidence intervals of the best-fit lines. **(A5, B5)** Proportion of spikes within cortical discharges plotted as a function of seizure duration in 4 age groups. Grey circles correspond to bilateral Dcx-KD rats, green circles correspond to bilateral Dcx-KD rats with chronically silenced SBH, and purple circles to bilateral Dcx-KD rats with chronically silenced NCx. **(C, D)** Cumming estimation plots illustrating the mean difference in the number of seizures (C) and in the proportion of spikes within cortical discharges (D) in bilateral Dcx-KD rats compared to bilateral Dcx-KD rats with chronically silenced SBH (green) and NCx (purple). Individual values are plotted on upper graphs, with vertical bars illustrating mean and 95%CI. On lower graphs, mean differences are plotted as bootstrap sampling distributions (shaded areas). Black dots with vertical error bars show mean difference and 95%CI. (For interpretation of the references to colour in this figure legend, the reader is referred to the web version of this article.)

discharges that, however, remained immature and relatively shorter.

To confirm that the two-step in utero electroporation procedure did not by itself contribute to the exacerbated epileptogenesis, we generated rats with NCx-targeted mCherry expression. We first bilaterally injected and electroporated plasmids encoding mCherry; then, 30 min later, we bilaterally injected and co-electroporated plasmids encoding GFP and Dcx shRNAs to create bilateral SBH. We then longitudinally monitored the age-related changes of epileptiform activity with the same experimental and analysis pipeline as used before. We found that Dcx-KD rats with NCx-targeted mCherry expression did not significantly differ from unmanipulated Dcx-KD rats for all seizure parameters studied (Supplementary Fig. 7).

Together, these observations reveal that an early, targeted suppression of neuronal excitability in either SBH or the NCx of bilateral Dcx-KD rats has a strikingly distinct impact on epileptogenesis, leading to either a favorable improvement of epilepsy progression, or to its exacerbation.

3.4. Suppression of neuronal excitability in the SBH or NCx of rats with active epilepsy is ineffective

We next investigated if suppressing neuronal excitability in the SBH or NCx could have a beneficial impact for seizures in Dcx-KD rats with active epilepsy. To gain a temporal control on the onset of excitability suppression, we used a molecular genetic approach enabling a conditional, 4-hydroxy-tamoxifen (4OHT)- and Cre-dependent expression of Kir2.1 channels (Supplementary Figs. 4, 5). With this approach, functional expression of Kir2.1 channels is induced with a single intraperitoneal injection of 4OHT (20 mg/kg), and is associated with significantly more hyperpolarized resting membrane potentials, as confirmed with patch-clamp recordings (mean difference, −13.40 mV, with 95% CI of mean [−17.31, −8.74], $p = 0.0005$, Mann-Whitney test, Supplementary Fig. 4).

We generated rats with conditional SBH-targeted Kir2.1 expression (referred to as rats with silenced SBH in Fig. 4A) using the same experimental approach as for the early silencing, but with different plasmid conditions (see Supplementary Fig. 5 C1, C2). To generate rats with conditional NCx-targeted Kir2.1 expression (referred to as rats with silenced NCx in Fig. 4B), we used two-step tripolar in utero electroporation and the plasmid conditions described in Supplementary Fig. 5 D1, D2.

Because bilateral Dcx-KD rats harbor fully developed SWDs from five months onward (see Fig. 2), we injected 4OHT in five-month-old rats. We then examined the short-term impact of the suppression of neuronal excitability by comparing seizure parameters one day before, and six days after 4OHT-induced Kir2.1 expression. In the two groups of rats, with either silenced SBH or NCx, we found no significant change in the numbers (Fig. 4 A1, B1), duration (Fig. 4 A2, B2) and amplitude of seizures (Fig. 4 A3, B3), or in the proportion of spikes within cortical discharges (Fig. 4 A4, B4). Together, these observations suggest that the approach has no beneficial impact in bilateral Dcx-KD rats with fully established epilepsy.

4. Discussion

The pathological substrate and dynamic changes leading to the development and progression of epilepsy remain largely elusive in malformations of cortical development. In the present study, we have characterized the development and age-related progression of epilepsy in a rat model of bilateral SBH with chronic spontaneous seizures. We report a gradual evolution of epilepsy with age, with prominent quantitative and qualitative age-related changes in seizure properties and patterns, accompanying the progression towards a fully developed pattern of SWD seen in adulthood. We further show that early and targeted manipulations of neuronal excitability in either the SBH or the overlying cortex have drastic effects on this age-related epilepsy progression. While an early suppression of SBH excitability has clear anti-epileptogenic effects, with a slower age-related increase of seizure numbers and a slower progression towards fully developed SWDs, the same manipulation in the normotopic cortex paradoxically exacerbates epileptogenesis. Last, we report that manipulating neuronal excitability with the same approach once epilepsy is established is ineffective, suggesting the existence of protracted critical periods for intervention.

Epilepsies are progressive brain network disorders, and especially those arising in childhood as a consequence of disrupted cortical

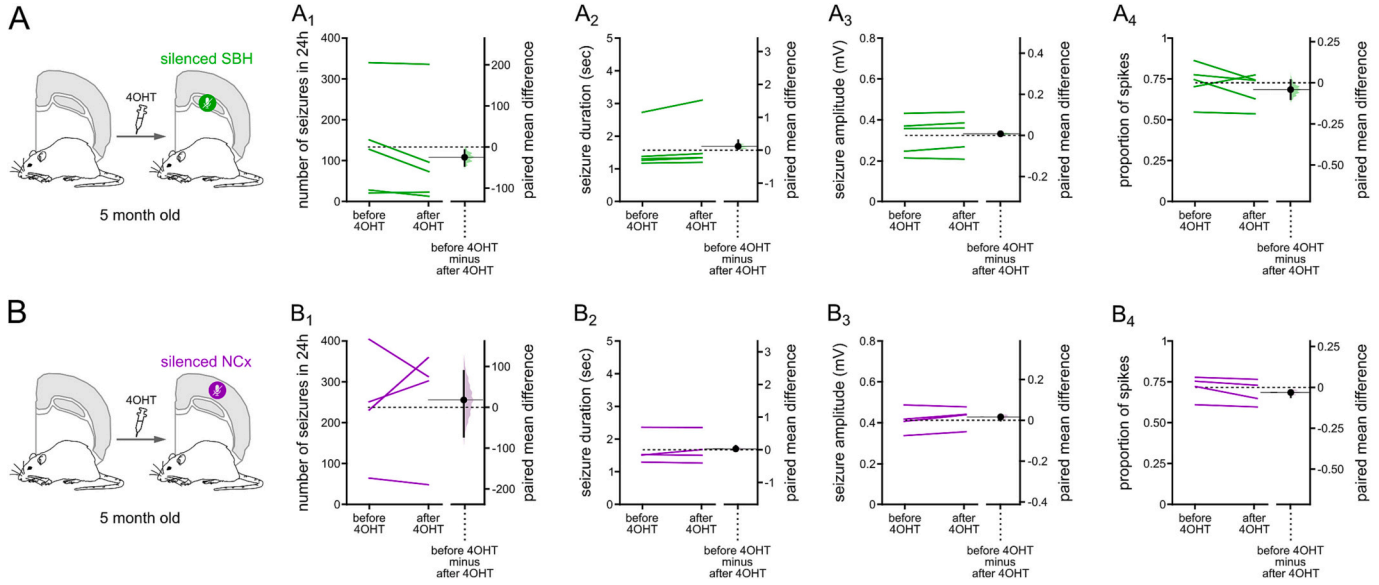

Fig. 4. Suppression of neuronal excitability in either the SBH or the normotopic cortex is ineffective for ameliorating seizure phenotype in 5-month-old bilateral Dcx-KD rats with active epilepsy. (A, B) Schematic views of the experimental design. **(A1-A4, B1-B4)** Gardner-Altman estimation plots of the paired mean difference in the number of seizures in 24 h (A1, B1), in the duration (A2, B2) and amplitude (A3, B3) of seizures, and in the proportion of spikes within cortical discharges (A4, B4) before and after suppression of neuronal excitability in the SBH (A1-A4) or in the NCx (B1-B4) of bilateral Dcx-KD rats, as induced by 4-hydroxy-tamoxifen (4OHT) injection. Each paired set of observations is connected by a line. The paired mean difference is plotted on a floating axis (right) as a bootstrap sampling distribution. Black dots with vertical error bars show mean difference and 95%CI.

development and aberrant circuit formation. Brains with SBH linked to DCX mutations in humans are mosaic (Di Donato et al., 2018), either caused by somatic mosaicism in male patients (D'Agostino et al., 2002) or related to X-inactivation in female patients (Bahi-Buisson et al., 2013). Accordingly, epilepsy in brains with SBH emerges and progresses in a context of ongoing cortical development, where both genetically normal and genetically altered neuronal populations interact together to form cortical networks. Hence, developing epileptogenic networks receive dual detrimental influences: those occurring as a direct consequence of the gene mutation, and those, likely reactive and non-genetic, arising indirectly or secondarily. In line with this, we have previously described in SBH rats both pathological alterations in the SBH (Ackman et al., 2009; Martineau et al., 2018), and secondary alterations in the overlying cortex (Petit et al., 2014; Ackman et al., 2009), several weeks before epilepsy onset. Further, we have reported developmental circuit changes in the normotopic cortex that were distinct depending on SBH location: decreased circuit excitability and connectivity strength in the cortex located above SBH, increased excitability and connectivity in the cortex lateral to SBH (Plantier et al., 2019). Such a complex combination comprising both local and distant changes suggests that brains with SBH harbor widespread circuit-level defects extending beyond the macroscopically visible heterotopia. This is in line with neuroimaging studies in patients with various types of MCDs, revealing widespread structural and functional circuit reorganization in focal cortical dysplasia (FCD) (Lee et al., 2021), in periventricular nodular heterotopia (PVNH) (Christodoulou et al., 2012) and in SBH (Sprugnoli et al., 2018).

In the present study, early manipulation of neuronal excitability has led to strikingly different consequences depending on the targeted area. These differences likely reflect distinct pathological mechanisms contributing to epileptogenesis in SBH – in which the causative mutation is the main contributor, and in the overlying cortex – in which secondary circuit-level reorganizations are prevailing as we demonstrated in Plantier et al. (Plantier et al., 2019) If both regions do concur to creating seizure-prone circuits, the weight of the SBH (and that of the causative gene) appears greater than that of the overlying cortex, as illustrated by a more favorable outcome of SBH-targeting manipulation. Although this remains to be tested, attenuating influences of the SBH by suppressing its excitability has likely prevented or attenuated both the pathogenic changes directly related to the causative gene, as well as the development and/or expansion of secondary circuit-level alterations. It would be equally important to clarify the possible contribution of altered patterns of neuronal firing in the SBH, and modified strength of functional network connectivity, to the ameliorated seizure outcomes. On the contrary, attenuating influences of the normotopic cortex was found insufficient, and, paradoxically, detrimental. This is not entirely unexpected, given that complex maladaptive circuit changes, combining both increased and decreased circuit excitability and connectivity, were found in the overlying cortex (Plantier et al., 2019). In this context, the destabilizing effects of local excitability changes may have led to an exacerbation of cortical imbalance in the normotopic cortex, further precipitating epileptogenesis. Whether larger numbers of cells with manipulated neuronal excitability in the normotopic cortex would lead to greater cortical imbalance and even more severe seizure phenotypes remains to be investigated.

Timing of intervention matters, and excitability suppression in rats with fully established epilepsy was found inefficient. Although speculative, we propose several explanations for this. First, with a continuing progression of network dysfunction as epilepsy progresses, the spatial extend of circuit alterations is likely far greater than that of the targeted circuits, precluding any beneficial impact. Second, the targeted circuits may potentially fall outside of the most epileptogenic regions, and their precise location and properties require clarification. Last, circuit-level alterations whose development and/or expansion can be limited with early interventions are unlikely to regress once development has ended. These hypotheses are in agreement with neuroimaging studies suggesting that the strength of the abnormal circuitry increases over time, as epilepsy progresses, in patients with grey matter heterotopia (Christodoulou et al., 2012). Therefore, the present work supports the notion that early corrective interventions, including surgical removal prior to drug-resistance, as recently proposed (Hale et al., 2022), may reduce morbidity, and improve neurocognitive outcomes.

Whether the favorably modified epileptogenesis described here has other beneficial effects remains to be investigated. The age of epilepsy onset in patients with SBH usually correlates with the severity of epilepsy and that of associated co-morbidities. Earlier ages of epilepsy onset, and larger proportions of drug-resistance, are observed in patients presenting with more severe intellectual and behavioral impairments, and with wider anatomical extend of SBH (Bahi-Buisson et al., 2013; Tanaka and Gleeson, 2008). We have previously reported that rats with unilateral SBH, and older ages of epilepsy onset, showed no cognitive impairments when tested prior to epilepsy onset (Martineau et al., 2019). Whether any cognitive alterations are associated with epilepsy progression, or are already present before epilepsy onset in rats with bilateral SBH would require further work.

In a large series of patients described by Bahi-Buisson et al. (Bahi-Buisson et al., 2013) 85% of SBH patients had seizure disorders, with epilepsy starting in infancy (35% of cases) or during childhood (45% of cases), and often associated with an evolution of seizure types or electrographic patterns with age. Here, we have described in SBH rats an age-related progression of electrographic patterns where epileptiform discharges finally shaped into fully developed SWDs. Longitudinal EEG monitoring of individual animals, as we have done here, is rarely performed over prolonged periods in rodent models of MCDs. Kao et al. (Kao et al., 2021) recently studied epileptogenesis in a rat model of Depdc5-related FCD type II, and documented a similar progression of immature electrographic patterns towards mature forms of cortical discharges. Using both intermittent and continuous EEG monitoring, they found that mature patterns gradually emerge from brief runs of SW complexes that progressively last longer, and finally morph into well-formed SWDs (Kao et al., 2021). Likewise, in the GAERS rat model of absence-type epilepsy, epileptiform activity gradually progresses during epileptogenesis. Oscillatory epileptiform discharges emerge first, become progressively intermingled with SW complexes, and finally shape into fully mature SWDs (Jarre et al., 2017). In GAERS rats, this progression towards mature discharges is accompanied by progressively increased excitability of cortical neurons and strengthening of local synaptic activity (Jarre et al., 2017), increased structural connectivity in the cortex (Studer et al., 2022), and altered developmental sequences of cortical wiring (Plutino et al., 2022). In bilateral SBH rats, the evolution of electrographic patterns likely engage similar mechanisms, and combines intrinsic and circuit excitability changes, modified excitation-inhibition ratio, and altered cortical connectivity, as we demonstrated previously (Plantier et al., 2019). Because we have observed a slower progression towards fully mature SWDs upon manipulation of excitability of both the SBH, and the normotopic cortex, this suggests that the two regions contribute to the maturation of electrographic patterns. Interestingly, reciprocal connections between the SBH and the normotopic cortex were described in SBH patients (Sprugnoli et al., 2018), in PVNH patients (Christodoulou et al., 2012; Nolan et al., 2020; Boulogne et al., 2022), and in murine models of SBH and PVNH (Vermoyal, Hardy et al., unpublished work) in keeping with this idea. Whether these reciprocal connections do contribute to the propagation or to the generalization of seizures in bilateral SBH rats would require further in vivo investigations with multi-site and multi-electrode recordings with precise targeting of the normotopic cortex and SBH.

To conclude, our longitudinal monitoring of epilepsy progression in rats with bilateral SBH reveals a gradual evolution of seizure properties and patterns during the course of epileptogenesis, before finally reaching a fully developed discharge pattern. Further, through timed and spatially targeted manipulation of neuronal excitability, we demonstrate that a complex combination of developmental alterations in both the SBH and the cortex contributes to epileptogenesis. Importantly, our

work also suggests that early corrective interventions may help attenuating the development or expansion of circuit-level alterations, with a positive impact on altered developmental trajectories. Because epileptogenesis and its treatment are priorities in epilepsy research and care (Galanopoulou et al., 2021), our work may contribute to a better understanding of the pathological substrate leading to epileptogenesis, and to the development of novel corrective interventions.

Supplementary data to this article can be found online at https://doi.org/10.1016/j.nbd.2023.106002.

Funding

This study was supported by the French National Agency for Research (SILENCEED, ANR-16-CE17-0013-01 to JBM), the European Community 7th Framework program (DESIRE, Health-F2–602531–2013 to A.R.), the *E*-Rare-3 action of ERA-NET for rare disease research (HETEROMICS, ERARE18–049, ANR-18-RAR3–0002-02 to JBM) and the ERA-NET funding scheme of NEURON for research projects of mental disorders (nEUROtalk, NEURON-061, ANR-18-NEUR-0003-01 to JBM). JBM and MM jointly received funding from France 2030, the French Government program managed by the French National Agency for Research (ANR-16-CONV-0001) and from Excellence Initiative of Aix-Marseille University - A*MIDEX.

CRediT authorship contribution statement

Delphine Hardy: Conceptualization, Methodology, Validation, Formal analysis, Data curation, Writing – review & editing, Visualization. **Emmanuelle Buhler:** Conceptualization, Methodology, Validation, Formal analysis, Data curation, Writing – review & editing. **Dmitrii Suchkov:** Conceptualization, Methodology, Software, Validation, Formal analysis, Data curation, Writing – review & editing, Visualization. **Antonin Vinck:** Methodology, Formal analysis, Writing – review & editing, Visualization. **Aurélien Fortoul:** Methodology, Formal analysis, Writing – review & editing, Visualization. **Françoise Watrin:** Conceptualization, Methodology, Validation, Writing – review & editing. **Alfonso Represa:** Conceptualization, Writing – review & editing, Funding acquisition. **Marat Minlebaev:** Conceptualization, Methodology, Writing – review & editing, Supervision, Funding acquisition. **Jean-Bernard Manent:** Conceptualization, Methodology, Validation, Formal analysis, Writing – original draft, Writing – review & editing, Visualization, Supervision, Project administration, Funding acquisition.

Declaration of Competing Interest

The authors report no competing interests.

Data availability

The data that support the findings of this study are available from the corresponding author, upon reasonable request.

Acknowledgements

We thank Dr. L. Cancedda for providing a prototype of the third electrode used for tripolar electroporation at the initial stage of the study, Dr. J. LoTurco for Dcx shRNAs plasmids and Dr. Y. Tagawa for Kir2.1 plasmids. We also thank the animal facility (PPGI, INMED, Marseille), the imaging facility (INMAGIC, INMED, Marseille), and the molecular and cellular biology facility (PBMC, INMED, Marseille).

References

Ackman, J.B., Aniksztejn, L., Crépel, V., et al., 2009 Jan 14. Abnormal network activity in a targeted genetic model of human double cortex. J. Neurosci. 29 (2), 313–327.

Andrey, P., Maurin, Y., 2005 Jun 30. Free-D: an integrated environment for three-dimensional reconstruction from serial sections. J. Neurosci. Methods 145 (1–2), 233–244.

Bahi-Buisson, N., Guerrini, R., 2013. Diffuse malformations of cortical development. Handb. Clin. Neurol. 111, 653–665.

Bahi-Buisson, N., Souville, I., Fourniol, F.J., et al., 2013 Jan. New insights into genotype-phenotype correlations for the doublecortin-related lissencephaly spectrum. Brain. 136 (Pt 1), 223–244.

Barkovich, A.J., Jackson Jr., D.E., Boyer, R.S., 1989 May. Band heterotopias: a newly recognized neuronal migration anomaly. Radiology. 171 (2), 455–458.

Boulogne, S., Pizzo, F., Chatard, B., et al., 2022 Apr. Functional connectivity and epileptogenicity of nodular heterotopias: a single-pulse stimulation study. Epilepsia. 63 (4), 961–973.

Burrone, J., O'Byrne, M., Murthy, V.N., 2002 Nov 28. Multiple forms of synaptic plasticity triggered by selective suppression of activity in individual neurons. Nature. 420 (6914), 414–418.

Christodoulou, J.A., Walker, L.M., Del Tufo, S.N., et al., 2012 Jun. Abnormal structural and functional brain connectivity in gray matter heterotopia. Epilepsia. 53 (6), 1024–1032.

D'Agostino, M.D., Bernasconi, A., Das, S., et al., 2002 Nov. Subcortical band heterotopia (SBH) in males: clinical, imaging and genetic findings in comparison with females. Brain. 125 (Pt 11), 2507–2522.

Di Donato, N., Timms, A.E., Aldinger, K.A., et al., 2018 Nov. Analysis of 17 genes detects mutations in 81% of 811 patients with lissencephaly. Genet Med. 20 (11), 1354–1364.

Dobyns, W.B., 2010 Feb. The clinical patterns and molecular genetics of lissencephaly and subcortical band heterotopia. Epilepsia. 51 (Suppl. 1), 5–9.

Galanopoulou, A.S., Löscher, W., Lubbers, L., et al., 2021 Jun. Antiepileptogenesis and disease modification: Progress, challenges, and the path forward-report of the preclinical working group of the 2018 NINDS-sponsored antiepileptogenesis and disease modification workshop. Epilepsia Open. 6 (2), 276–296.

Guerrini, R., Dobyns, W.B., 2014 Jul. Malformations of cortical development: clinical features and genetic causes. Lancet Neurol. 13 (7), 710–726.

Hale, A.T., Chari, A., Scott, R.C., et al., 2022. Expedited epilepsy surgery prior to drug resistance in children: a frontier worth crossing? Brain. https://doi.org/10.1093/brain/awac275. Published online 27 July.

Ho, J., Tumkaya, T., Aryal, S., Choi, H., Claridge-Chang, A., 2019 Jul. Moving beyond P values: data analysis with estimation graphics. Nat. Methods 16 (7), 565–566.

Jarre, G., Altwegg-Boussac, T., Williams, M.S., et al., 2017 Sep 1. Building up absence seizures in the somatosensory cortex: from network to cellular epileptogenic processes. Cereb. Cortex 27 (9), 4607–4623.

Kao, H.Y., Hu, S., Mihaylova, T., et al., 2021 May. Defining the latent period of epileptogenesis and epileptogenic zone in a focal cortical dysplasia type II (FCDII) rat model. Epilepsia. 62 (5), 1268–1279.

Kenny, M., Schoen, I., 2021 Jul 15. Violin SuperPlots: visualizing replicate heterogeneity in large data sets. Mol. Biol. Cell 32 (15), 1333–1334.

Lee, D.A., Lee, H.J., Kim, H.C., Park, K.M., 2021 Aug 27. Alterations of structural connectivity and structural co-variance network in focal cortical dysplasia. BMC Neurol. 21 (1), 330.

Leventer, R.J., Guerrini, R., Dobyns, W.B., 2008. Malformations of cortical development and epilepsy. Dialogues Clin. Neurosci. 10 (1), 47–62.

Martineau, F.S., Sahu, S., Plantier, V., et al., 2018 Aug 1. Correct laminar positioning in the neocortex influences proper dendritic and synaptic development. Cereb. Cortex 28 (8), 2976–2990.

Martineau, F.S., Fournier, L., Buhler, E., et al., 2019 May 15. Spared cognitive and behavioral functions prior to epilepsy onset in a rat model of subcortical band heterotopia. Brain Res. (1711), 146–155.

Matsumoto, N., Leventer, R.J., Kuc, J.A., et al., 2001 Jan. Mutation analysis of the DCX gene and genotype/phenotype correlation in subcortical band heterotopia. Eur. J. Hum. Genet. 9 (1), 5–12.

Mizuno, H., Hirano, T., Tagawa, Y., 2007 Jun 20. Evidence for activity-dependent cortical wiring: formation of interhemispheric connections in neonatal mouse visual cortex requires projection neuron activity. J. Neurosci. 27 (25), 6760–6770.

Moustaki, K., Buhler, E., Martinez, R., Watrin, F., Represa, A., Manent, J.B., 2019 Oct 18. Size of subcortical band heterotopia influences the susceptibility to hyperthermia-induced seizures in a rat model. Front. Cell. Neurosci. (13), 473.

Nolan, R.L., Brandmeir, N., Tucker, E.S., et al., 2020 Feb 1. Functional and resting-state characterizations of a periventricular heterotopic nodule associated with epileptogenic activity. Neurosurg. Focus. 48 (2), E10.

Petit, L.F., Jalabert, M., Buhler, E., et al., 2014 Sep. Normotopic cortex is the major contributor to epilepsy in experimental double cortex. Ann. Neurol. 76 (3), 428–442.

Pitkänen, A., Nehlig, A., Brooks-Kayal, A.R., et al., 2013 Aug. Issues related to development of antiepileptogenic therapies. Epilepsia. 54 (Suppl 4(0 4)), 35–43.

Plantier, V., Watrin, F., Buhler, E., et al., 2019 Sep 13. Direct and collateral alterations of functional cortical circuits in a rat model of subcortical band heterotopia. Cereb. Cortex 29 (10), 4253–4262.

Plutino, S., Laghouati, E., Jarre, G., Depaulis, A., Guillemain, I., Bureau, I., 2022. Barrel cortex development lacks a key stage of hyperconnectivity from deep to superficial layers in a rat model of Absence Epilepsy. bioRxiv. [Preprint]. https://doi.org/10.1101/2022.03.18.484944.

Represa, A., 2019 Mar 29. Why malformations of cortical development cause epilepsy. Front. Neurosci. (13), 250.

Sahu, S., Buhler, E., Vermoyal, J.C., Watrin, F., Represa, A., Manent, J.B., 2019 Feb. Spontaneous epileptiform activity in a rat model of bilateral subcortical band heterotopia. Epilepsia. 60 (2), 337–348.

Sprugnoli, G., Vatti, G., Rossi, S., et al., 2018 Jun 12. Functional connectivity and genetic profile of a "double-cortex"-like malformation. Front. Integr. Neurosci. (12), 22.
Studer, F., Jarre, G., Pouyatos, B., et al., 2022 Jun 30. Aberrant neuronal connectivity in the cortex drives generation of seizures in rat absence epilepsy. Brain. 145 (6), 1978–1991.
Tanaka, T., Gleeson, J.G., 2008. Subcortical laminar (band) heterotopia. Handb. Clin. Neurol. 87, 191–204.
White, B., Osterwalder, T., Keshishian, H., 2001 Dec 11. Molecular genetic approaches to the targeted suppression of neuronal activity. Curr. Biol. 11 (24), R1041–R1053.